Journal of Alloys and Compounds 708 (2017) 605–611

Contents lists available at ScienceDirect

Journal of Alloys and Compounds

journal homepage: http://www.elsevier.com/locate/jalcom

Effect of synthesis temperature on the magneto-electrochemical properties of $LaFe_{0.9}Co_{0.1}O_3$ nanoparticles

Sumalin Phokha [a, *], Sitchai Hunpratub [a], Brian Usher [a], Narong Chenlek [b], Atipong Bootchanont [c], Santi Maensiri [d], Prinya Chindaprasirt [e]

[a] Department of Physics, Faculty of Science, Udon Thani Rajabhat University, Udon Thani, 41000, Thailand
[b] Synchrotron Light Research Institute (Public Organization), 111 University Avenue, Muang District, Nakhon Ratchasima, 30000, Thailand
[c] Division of Physics, Faculty of Science and Technology, Rajamangala University of Technology Thanyaburi (RMUTT), Pathumthani, 12110, Thailand
[d] School of Physics, Institute of Science, Suranaree University of Technology, Nakhon Ratchasima, 30000, Thailand
[e] Sustainable Infrastructure Research and Development Center, Department of Civil Engineering, Faculty of Engineering, Khon Kaen University, Khon Kaen, 40002, Thailand

ARTICLE INFO

Article history:
Received 21 October 2016
Received in revised form
14 January 2017
Accepted 4 March 2017
Available online 7 March 2017

Keywords:
$LaFe_{0.9}Co_{0.1}O_3$
Ferromagnetic properties
Electrochemical properties
X-ray absorption near edge spectroscopy (XANES)
X-ray photoelectron spectroscopy (XPS)

ABSTRACT

Orthoferrites $LaFe_{0.9}Co_{0.1}O_3$ nanoparticles were synthesized by a polymer pyrolysis method and calcined at 700, 800, 900 and 1000 °C for 3 h in air. The structure, morphology, valence states, magnetic and charge-discharge properties of the nanoparticles were characterized using X-ray diffraction (XRD), transmission electron microscopy (TEM), X-ray absorption near edge structure (XANES), X-ray photoelectron spectroscopy (XPS), vibrating sample magnetometer (VSM) and a potentiostat/galvanostat electrochemical cell system, respectively. Rietveld analysis confirmed the presence of a single phase and that the perovskite lattice exhibited an orthorhombic distortion. The average crystallite sizes increased from 32 ± 6 to 78 ± 6 nm with increasing calcination temperature. From the XANES and XPS results, the valence states of Fe and Co ions in samples were Fe^{3+}, Co^{3+} and Co^{2+} and the ratio of the number of Co^{3+} and Co^{2+} states varied between samples. All samples exhibited ferromagnetic behavior at room temperature with a maximum magnetization value of 1.0 emu/g for the sample calcined at 900 °C. The relationship between the Co^{3+}/Co^{2+} ratio and the origin of the ferromagnetism is discussed. The highest discharge capacity of electrodes made from $LaFe_{0.9}Co_{0.1}O_3$ nanoparticles was 1150 mAh/g, suggesting the high surface area to volume ratios of the nanoparticles.

1. Introduction

Orthoferrites have the formula $XFeO_3$ where X represents an alkali or rare earth ion such as Bi, La, Pr, Nd, Sm, Eu and Gd etc [1–9] which sits on an A site (tetrahedral) within the oxygen fcc sublattice and the B sites (octahedral) are occupied by Fe ions. The nanocrystal forms of these materials have attracted much attention because their physical and chemical properties are significantly different from their bulk counterparts due to their high surface area to volume ratios. Some of these properties are important in various applications such as solid oxide fuel cells, photocatalysts, chemical sensors, batteries and super-capacitors [1,6]. These materials also show promise in application such as magnetic field sensors, magneto-optical and spintronic devices [2,3,6–8] due to their room temperature (RT) ferromagnetic (FM) properties.

The substitution of various transition metals (TM) onto $LaFeO_3$ A and/or B sites and the preparation of nanometer-sized particles has produced improvements in its structural, magnetic and electrochemical properties. For example, RT-FM behavior has been reported following TM substitution on A sites in materials such as $La_{1-x}Zn_xFeO_3$ [10], $La_{1-x}Ga_xFeO_3$ [11] and $La_{0.5}Al_{0.5}FeO_3$ [12] as well as TM substitution on B sites in materials such as $LaFe_{1-x}Ti_xO_3$ [13], $LaFe_{1-x}Cr_xO_3$ [14], $LaFe_{0.9}Mn_{0.1}O_3$ [15] and $LaFe_{0.75}Mn_{0.25}O_3$ [16] or both A and B sites, for example in $La_{0.8}Sr_{0.2}Fe_{1-x}Cu_xO_{3-w}$ [17]. A structural transition from orthorhombic to rhombohedral can change a materials magnetic behavior, for example higher Mn concentrations in $LaFe_{1-x}Mn_xO_3$ ($x > 0.5$) results in a rhombohedral structure which exhibits antiferromagnetic behavior [16]. In another example Lim et al. [18] have reported that polycrystalline $LaFeO_3$ has a charge-discharge current density of approximately

* Corresponding author.
E-mail address: sumalinphokha@gmail.com (S. Phokha).

http://dx.doi.org/10.1016/j.jallcom.2017.03.041
0925-8388/

50 mAh/g at RT, whereas $La_{1-x}Sr_xFeO_3$ showed more than 500 mAh/g at 60 °C [19]. To date there have been no studies of the magnetic and electrochemical properties following Co ion substitution on B sites within a $LaFeO_3$ host. It is therefore of interest to study these properties in $LaFe_{1-x}Co_xO_3$ nanoparticles to further our scientific understanding of this class of materials and also for their potential applications.

In this work, Co-doped $LaFeO_3$ ($LaFe_{0.9}Co_{0.1}O_3$) nanoparticles were prepared by the polymer pyrolysis method and their crystallinity and morphology were characterized by XRD and TEM. The valence states of Fe and Co ions were studied by XANES and XPS from which the ratio of the number of Co^{3+} and Co^{2+} ions in the samples could be determined. The magnetic properties of the nanoparticles were investigated using a VSM. The charge-discharge capacity of electrodes made from $LaFe_{0.9}Co_{0.1}O_3$ were measured using a potentionstat/galvanostat electrochemical cell system.

2. Experimental

Nanoparticle of $LaFe_{0.9}Co_{0.1}O_3$ was synthesized by the polymer pyrolysis method according to procedures established in previous work [2,20–24]. Briefly, 0.006 mol of $La(NO_3)_3.6H_2O$ (Aldrich), $Fe(NO_3)_3.9H_2O$ (Kanto), $Co(NO_3)_2.6H_2O$ (Aldrich) and 70 ml of acrylic acid ($C_3H_4O_2$) were dissolved in deionized water to promote polymerization after which the precursor solution was heated to 30 °C and stirred until it dried. The dried precursor was then pre-calcined in a furnace at 400 °C for 2 h to form a polyacrylate salt which was then calcined at temperatures of 700, 800, 900 and 1000 °C for 3 h in air to obtain $LaFe_{0.9}Co_{0.1}O_3$ nano-crystals.

The prepared samples were characterized using XRD, TEM, XANES, XPS and VSM.

An XRD system (Bruker D2 Phaser) equipped with a Cu anode source (λ = 0.154184 nm) and TEM (Ziess, EM902) were used to study the phases, crystal sizes and morphology of the $LaFe_{0.9}Co_{0.1}O_3$ samples. XANES and XPS experiments to allow determination of the Fe and Co valence states were performed in transmission mode on the BL5.2 and BL5.1 beam lines at the Synchrotron Light Research Institute in Nakhon Ratchasima, Thailand, respectively. Magnetic hysteresis measurements were performed at room temperature using a VSM (Versa Lab, Quantum Design) with applied fields between −10000 and 10000 Oe. Field cooling mode measurements were made using the same equipment, with an applied external field of 500 Oe and sample temperatures between 50 and 390 K. Charge–discharge measurements were made at RT using a potentionstat/galvanostat electrochemical cell system (Austin, TX).

3. Results and discussion

Fig. 1 shows the XRD patterns obtained from the $LaFe_{0.9}Co_{0.1}O_3$ samples calcined at various temperatures. The peaks match with those of the orthorhombic structure of $LaFeO_3$ according to the JCPDS standard 88-0641 (space group *Pnma*) for all samples. There are no diffraction peaks associated with impurity phases, indicating the formation of a pure phase with Co doping. The goodness of fit (GOF, χ^2) was found to be in the range of 1.1–1.5 as shown in Table 1. It can also be seen from Table 1 that the crystallite sizes (D_{XRD}) calculated using Scherrer's equation increase from 32 ± 6 to 78 ± 6 nm, for calcination temperatures from 700 to 1000 °C. One of the effects of increasing the calcination temperature was to create significantly larger crystals as a result of agglomeration. Because increasing calcination temperature was also associated with a narrowing of the XRD peaks it suggests there may have been some recrystallization following agglomeration [20]. However, there was no significant difference in the D_{XRD} for Co-doped samples compared to those of 34.8 ± 1.5–74.0 ± 2.8 nm for undoped

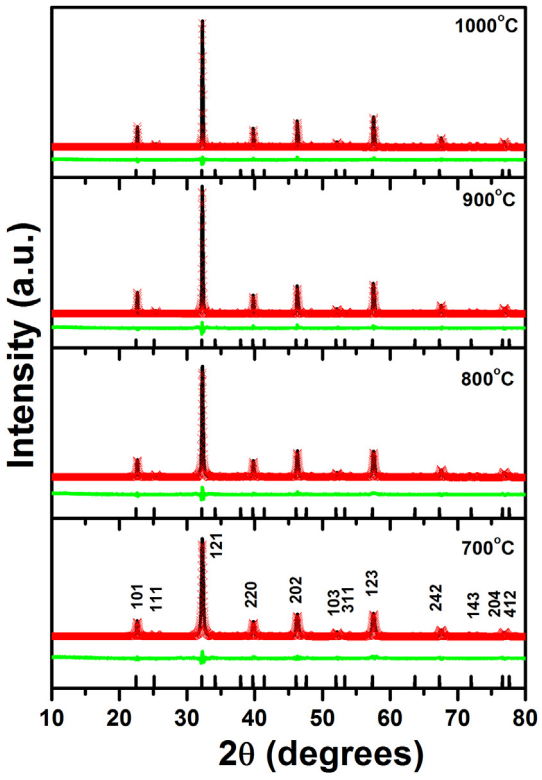

Fig. 1. XRD patterns obtained from $LaFe_{0.9}Co_{0.1}O_3$ samples calcined at various temperatures for 3 h in air. The measured data are indicated by the dots and the calculated data by solid lines overlaying the data. The lower curve in each window shows the difference between the observed and calculated data and the vertical bars are the peak positions obtained from the JCPDS standard 88-0641 for $LaFeO_3$.

samples at the same calcination temperatures [2]. This is possibly due to the substitution of the Fe^{3+} sites by the small amount Co ions (10 at %), leading to a small change in the lattice parameter and the crystallite sizes which is in good agreement with earlier reports [23]. This increase of calcination temperatures is observed that

Table 1
Summary of crystallite sizes as measured by XRD line broadening (D_{XRD}) and TEM direct imaging (D_{TEM}), parameters as calculated by Rietveld analysis, Gaussian fits of XPS spectra, saturated magnetization (M_S) at RT, remanence magnetization (M_R) and coercivity (H_C) of $LaFe_{0.9}Co_{0.1}O_3$ nanoparticles calcined at various temperatures for 3 h in air.

Parameter	Calcined temperatures			
	700 °C	800 °C	900 °C	1000 °C
D_{XRD} (nm)	32 ± 6	46 ± 4	65 ± 4	78 ± 6
D_{TEM} (nm)	51 ± 5	81 ± 7	172 ± 20	258 ± 20
a (Å)	5.551(1)	5.543(7)	5.543(4)	5.541(2)
b (Å)	7.829(9)	7.832(9)	7.832(4)	7.829(2)
c (Å)	5.546(1)	5.545(8)	5.545(4)	5.545(3)
Volume (Å^3)	241.03	240.72	240.70	240.56
GOF (χ^2)	1.1	1.3	1.5	1.4
Rp (%)	8.7	9.3	9.4	9.6
Rwp (%)	11.6	12.6	13.4	13.8
Peak Position (eV)				
Co^{3+}	780.5/795.2	780.2/794.7	780.2/794.8	–
Co^{2+}	782.4/796.4	782.4/796.5	782.1/797.0	–
Peak Area (eV)				
Co^{3+}	695.4/168.2	875.5/217.6	589.3/321.5	–
Co^{2+}	585.3/62.1	755/150.4	457.9/76.0	–
Percentage of Co^{3+} (%)	57.2	54.7	63.1	–
Percentage of Co^{2+} (%)	42.8	45.3	36.9	–
M_S (emu/g)	0.67	0.55	1.00	0.98
M_R (emu/g)	0.21	0.19	0.48	0.41
H_C (Oe)	1016	1003	850	620